

# Random-Matrix Theory: Distribution of Mesoscopic Supercurrents through a Chaotic Cavity

Markus Garst<sup>1</sup> and Thilo Kopp<sup>2</sup>

<sup>1</sup> TKM, Universität Karlsruhe, D-76128 Karlsruhe, Germany

<sup>2</sup> EP VI, EKM, Universität Augsburg, D-86135 Augsburg, Germany

*We investigate the distribution of the supercurrent through a chaotic quantum dot which is strongly coupled to two superconductors when the Thouless energy is large compared to the superconducting energy gap. The distribution function of the critical currents  $\rho(I_c)$  is known to be Gaussian in the limit of large channel number,  $N \rightarrow \infty$ . For  $N = 1$ , we present an analytical low-temperature expression for this distribution function, valid both in the presence and in the absence of time-reversal symmetry. It connects directly the distribution of transmission coefficients to the distribution of critical currents. The case of arbitrary channel number ( $N \geq 2$ ) is discussed numerically, and for small critical currents analytically.*

*PACS numbers: 73.20.Dx, 74.50.+r, 74.60.Jg, 74.80.Fp, 73.20.Dx, 85.25.Cp.*

## 1. INTRODUCTION

Electronic transport through mesoscopic structures with system size  $L$  smaller than the electron phase relaxation length  $L_\phi$  has become a unique “playground” to study quantum interference effects.<sup>1,2</sup> An intriguing phenomenon which convincingly presents the essence of quantum interference in diffusive electronic transport are the universal conductance fluctuations (UCF). Their size is of the order of  $e^2/h$ , independent of sample geometry or the details of the realization of disorder, provided that the electronic system stays in the diffusive transport regime. UCF were first considered in a diagrammatic approach,<sup>4,5</sup> and then soon discussed within random-matrix theory (RMT)<sup>6,7</sup> which Imry<sup>8</sup> had proposed to apply for this class of problems. UCF were observed as magneto-finger-prints in mesoscopic wires (see

## M. Garst and T. Kopp

the measurement of conductance fluctuations in gold wires by Washburn and Webb<sup>9</sup>).

The superconducting analogue of UCF in normal conducting wires are supercurrent fluctuations in chaotic SNS-Josephson point contacts, as put forward by Beenakker.<sup>10,11</sup> The sample-to-sample fluctuations of the critical current  $I_c$  depend only on the gap in the single particle spectrum:

$$\text{rms } I_c \equiv \sqrt{\langle I_c^2 \rangle - \langle I_c \rangle^2} = c \frac{e\Delta}{\hbar} \quad (1)$$

with a numerical coefficient  $c$  of order unity. Here,  $\Delta$  is the bulk gap, and the junction extension is assumed to be small compared to the coherence length. Again, the fluctuations are universal in the sense that they do not depend on junction parameters like, for example, the degree of disorder or the junction geometry. These universal supercurrent fluctuations still have to be verified experimentally.

The realization depends on several conditions. First of all, the dynamics of the junction should be chaotic either due to impurities or boundary scattering. For example, for a diffusive junction, the junction length  $L$  (which is to be taken as the separation of SN interfaces) has to be much larger than the mean free path  $l$  in the normal-conducting part of the junction,  $l \ll L$ . Secondly, to ensure universality, the superconducting energy has to be the only low energy scale. This amounts to the criterion that the Thouless energy  $E_c = \hbar/\tau_d$  is much larger than the maximum gap in the energy spectrum,  $E_c \gg \Delta$ , where  $\tau_d$  is the mean dwell time of electrons or holes in the junction. For a diffusive junction, this condition of a short dwell-time is fulfilled if  $L$  is much smaller than the coherence length,  $L \ll \xi$ , where  $\xi = (\xi_o l)^{1/2}$  is the diffusive coherence length,  $\xi_o = \hbar v_F/(\pi\Delta)$ , and  $v_F$  is the Fermi velocity. Moreover, the number  $N$  of transverse modes at the Fermi level which propagate through the junction, has to be large to allow an expansion in the “dimensionless inverse conductance”  $(2e^2/h)/\langle G \rangle$  and thus to prove that the numerical coefficient  $c$  in Eq. (1) is indeed independent of  $N$ .<sup>11</sup>

Physically, (a) multiple Andreev reflection at the interfaces,<sup>13</sup> and (b) the statistics of the transmission eigenvalues lead to the universal fluctuations, Eq. (1). Thereby, (a) is responsible for the formation of current carrying bound (Andreev-) states in the junction. In the short dwell-time regime, only one Andreev state per channel exists. As a consequence, the supercurrent  $I(\phi)$  is a linear statistic<sup>14</sup> on the normal-region transmission coefficients  $T_n$  ( $1 \leq n \leq N$ ), independent of all junction parameters. However, the critical current  $I_c \equiv \max I(\phi) \equiv I(\phi_c)$  is in general not a linear statistic on  $T_n$  since the phase  $\phi_c$  at which the supercurrent is maximal depends on all the transmission coefficients. Beenakker showed that  $I(\phi_c)$  approximately obeys

## RMT: Distribution of Mesoscopic Supercurrents . . .

a linear statistic to within a correction of order  $1/N$ , where  $N$  is the number of channels. From the statistical properties of the transmission eigenvalues  $T_n$  it is known that the fluctuations of a linear statistic are of order unity and thus are universal, Eq. (1).

In this work we consider a Josephson junction where a chaotic quantum dot is strongly coupled to two superconductors. It is known that the scattering matrix of the normal conducting dot in this case belongs to the “circular unitary ensemble” (CUE) of RMT.<sup>15</sup> The case of a weakly coupled junction was considered elsewhere.<sup>16</sup> We are especially interested in the fluctuations of the supercurrent if the number of conducting channels in the normal chaotic region,  $N$ , is small. This implies that the critical current does not obey a linear statistic. Nevertheless, we expect that the sample-to-sample fluctuations are still determined by the relation Eq. (1). However, the prefactor  $c$  will now be weakly dependent on the number of channels  $N$ . More relevant is the question of how the full distribution of critical currents,  $\rho(I_c)$ , will behave when we transit from a situation with no level repulsion ( $N = 1$ ) to the scenarios with level repulsion ( $N \geq 2$ ). Certainly, the two situations differ qualitatively. For  $N \rightarrow \infty$  the distribution is a Gaussian.<sup>17</sup> For a single-channel junction, the literature does not provide a numerical or analytical result, to our knowledge. The missing level repulsion will move the center of the distribution to a lower value of  $I_c$ , the details of which should depend on the chosen ensemble. Finally, the case of a small number of channels is intriguing because it will interpolate between these two qualitatively incompatible situations — no level repulsion versus repulsion between many levels.

Although a Josephson junction with these properties has not yet been realized, neither for a small nor for a large number of channels, the microfabrication of point contacts with a small number of channels is already feasible (for example, see Refs. 18,19,20); and findings like the conductance quantization, related to the Friedel sum rule,<sup>21</sup> open new possibilities for the research of correlation effects in nano-scale structures. Chaotic point contacts are now within reach of experiments. The investigation of the interference of diffusion and Coulomb interaction should soon be possible, and we expect new exciting physics to emerge in these systems.

## 2. MODEL

In the recent 15 years, RMT has become a tool with which electronic transport through disordered mesoscopic systems can be studied very efficiently. It builds on the statistical independence of the elements of, e.g. the

scattering matrix and directly implements the symmetry of this matrix. As an excellent review by Beenakker<sup>15</sup> on this topic is available, we will only motivate some of the basic results in this section. We are going to apply RMT to the normal region of the SNS contact. The model which we use for the SNS contact was suggested in Ref. 11. However, we will extend the previous considerations to heterogeneous contacts.

### 2.1. Random Matrix Theory for the Chaotic Region

The critical current through an SNS-junction is determined by a specific realization of a random potential in the normal region which is the origin of the mesoscopic fluctuations. Interaction effects between the electrons in the normal metal are not taken into account, neither is spin-orbit coupling.

Concerning the interface between the superconducting and the normal regions, two scenarios have to be distinguished: the case of weak coupling, realized for instance by tunneling barriers<sup>16</sup> and the case of strong coupling with ideal, impurity-free leads at  $z_1$  and  $z_2$  (see Fig. 1). In the latter case, the scattering matrix  $\mathcal{S}$  is a unitary random matrix with eigenvalues uniformly distributed on the complex unit circle,<sup>15,23</sup> and the corresponding ensemble is referred to as CUE. In this article we will consider only the circular ensemble, that is, we stay in the strong coupling regime. Furthermore, we assume the Thouless energy to be much larger than the gap,  $E_c \gg \Delta$ . In this limit, which was named “short dwell-time regime” in Ref. 16, the energy dependence of the scattering matrix can be neglected.

On the other hand, the dwell-time  $\tau_d$  of electrons and holes in the chaotic region — with energies close to the Fermi level — has to be sufficiently large so that RMT is applicable. The dwell-time  $\tau_d$  should be larger than the time scale  $\tau_{\text{erg}}$  at which ergodicity sets in, where  $\hbar/\tau_{\text{erg}} = \hbar v_F \min\{l, L\}/L^2$ .

The scattering matrix  $\mathcal{S}$  has the block structure

$$\mathcal{S} = \begin{pmatrix} r & t' \\ t & r' \end{pmatrix}, \quad (2)$$

with the reflection matrices  $r, r'$  and the transmission matrices  $t, t'$ , all of which are  $N \times N$  matrices. The number of propagating modes in each of the two leads is  $N$ . Current conservation implies that the scattering matrix is unitary:  $\mathcal{S}^{-1} = \mathcal{S}^\dagger$ , and a “polar decomposition” is possible:<sup>7,22</sup>

$$\mathcal{S} = \begin{pmatrix} U & 0 \\ 0 & V \end{pmatrix} \begin{pmatrix} -\sqrt{1-T} & \sqrt{T} \\ \sqrt{T} & \sqrt{1-T} \end{pmatrix} \begin{pmatrix} U' & 0 \\ 0 & V' \end{pmatrix}, \quad (3)$$

where a  $N \times N$  diagonal matrix  $T = \text{diag}(T_1, T_2, \dots, T_N)$  has been introduced. The transmission eigenvalues  $T_n$  are the eigenvalues of the matrix

# RMT: Distribution of Mesoscopic Supercurrents ...

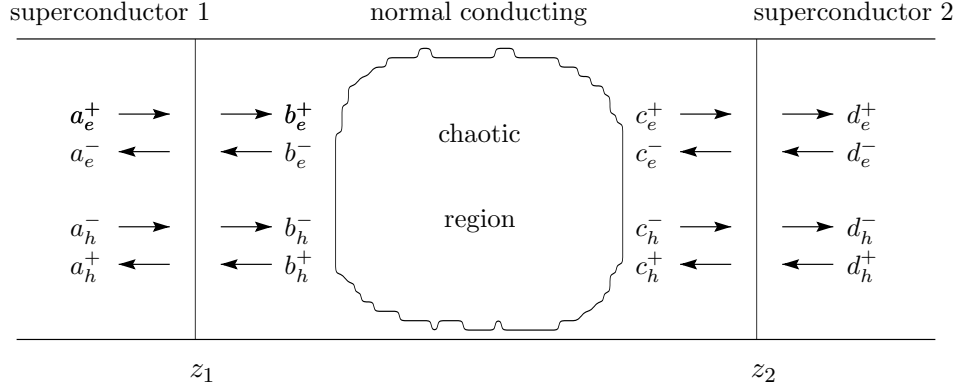


Fig. 1. Junction geometry and definition of scattering amplitudes for particles (e) and holes (h).

product  $tt^\dagger = t't'^\dagger$ . The four unitary  $N \times N$  matrices  $U, U'$  and  $V, V'$  are to be interpreted as “phase factors”. In the case of time-reversal symmetry the scattering matrix is unitary and symmetric,  $\mathcal{S} = \mathcal{S}^T$ , which implies that also  $U' = U^T$  and  $V' = V^T$  hold (“circular orthogonal ensemble” (COE)).

For statistical averaging we need the Haar measure  $\mu$  which can be determined for the above polar decomposition as<sup>23,24</sup>

$$d\mu(\mathcal{S}) = J(\{T_n\}) \prod_{\alpha} d\mu(U_{\alpha}) \prod_i dT_i. \quad (4)$$

The Jacobian is the probability distribution  $P(\{T_n\})$  of the transmission eigenvalues (up to a normalization constant  $c_N$ ); it is given by

$$J(\{T_n\}) = \prod_{n < m} |T_n - T_m|^{\beta} \prod_k T_k^{-1+\beta/2} = c_N P(\{T_n\}) \quad (5)$$

Here,  $\beta$  is the ensemble parameter—which numbers the degrees of freedom of the matrix elements of  $\mathcal{S}$ :

$$\begin{aligned} \beta &= 1 & \text{COE} & \text{system with time-reversal symmetry} \\ \beta &= 2 & \text{CUE} & \text{no time-reversal symmetry} \end{aligned} \quad (6)$$

for the two cases considered in this paper. The set of independent unitary matrices in the Haar measure (4) is  $\{U_{\alpha}\} = \{U, V, U', V'\}$  for  $\beta = 2$ , and  $\{U_{\alpha}\} = \{U, V\}$  for  $\beta = 1$ . For the purpose of interpreting the probability

## M. Garst and T. Kopp

distribution (5) it has become popular to write it in the form of a Gibbs distribution

$$P(\{T_n\}) = \frac{1}{c_N} \exp \left( \beta \sum_{n < m} \ln |T_n - T_m| - \beta \sum_k V(T_k) \right), \quad (7)$$

with the “one-particle” potential  $V(T_k) = (1/\beta - 1/2) \ln T_k$  and a “two-particle” logarithmic repulsion.

### 2.2. Scattering Matrix of the SNS Junction

Here we follow the approach pioneered by Beenakker,<sup>11</sup> and extend it in order to include the case of heterogeneous junctions.<sup>12</sup> The details of how to set up the Bogoliubov-de Gennes (BdG) equation for this type of junction are found in the cited paper and in Ref. 25, and will not be repeated here.

The S-matrix of the complete junction,  $\mathbf{S}_{\text{SNS}}$ , connects in- with outgoing amplitudes of the electronic wave function in the superconductors. The components of the wave function are defined in Fig. 1; for example, we have for the outgoing amplitudes  $N$  components  $a_e^-$  for electron-like quasiparticles running from the interface  $z_1$  to the left and  $N$  components  $d_e^+$  for electron-like quasiparticles running from the interface  $z_2$  to the right. Andreev reflection mixes particle with hole components, and therefore the corresponding hole-like quasiparticles with  $N$  components  $a_h^+$  and  $d_h^-$  have to be included in the scattering process. The  $4N \times 4N$ -matrix  $\mathbf{S}_{\text{SNS}}$  is now defined through

$$\begin{pmatrix} a_e^- \\ d_e^+ \\ a_h^+ \\ d_h^- \end{pmatrix} = \mathbf{S}_{\text{SNS}} \begin{pmatrix} a_e^+ \\ d_e^- \\ a_h^- \\ d_h^+ \end{pmatrix}. \quad (8)$$

The matrix  $\mathbf{S}_{\text{SNS}}$  is actually constructed from more basic  $4N \times 4N$  S-matrices,  $\mathbf{S}_N$  and  $\mathbf{S}_A$ . The matrix  $\mathbf{S}_N$  is formed by the scattering matrices for electrons and holes in the normal, disordered region:

$$\mathbf{S}_N(E) = \begin{pmatrix} \mathcal{S}(E) & 0 \\ 0 & \mathcal{S}^*(-E) \end{pmatrix} \quad (9)$$

where  $E$  is the energy relative to the Fermi energy. The matrix  $\mathbf{S}_A$ , defined by

$$\mathbf{S}_A(E) = \begin{pmatrix} 0 & e^{-i(\varphi(E) - \Phi)} \\ e^{-i(\varphi(E) + \Phi)} & 0 \end{pmatrix} \quad (10)$$

### RMT: Distribution of Mesoscopic Supercurrents ...

is the scattering matrix for Andreev reflections at both NS interfaces. The off-diagonal structure originates in the fact that Andreev reflection transforms an electron into a hole. The transformation is supplemented by two phase shifts: one from the penetration of the wave function into the superconductors

$$\varphi = \begin{pmatrix} \varphi_1 \mathbf{1}_N & 0 \\ 0 & \varphi_2 \mathbf{1}_N \end{pmatrix} \quad (11)$$

where  $\mathbf{1}_N$  is the  $N \times N$  unit matrix, and

$$\varphi_j = -i \ln \left( \frac{E}{\Delta_j} + \sqrt{\left( \frac{E}{\Delta_j} \right)^2 - 1} \right). \quad (12)$$

The  $\Delta_j$  are the respective Bogoliubov quasiparticle energy gaps of the two superconductors. We use rigid boundary conditions with step-like gaps at the SN-interfaces. This is approximately valid for the considered case that the extension of the junction is much smaller than the coherence length in the bulk superconductor.<sup>26</sup> The second contribution to the phase shift in (10) is the phase  $\phi_{1,2}$  acquired from the pair potential in the superconductors which has the matrix form

$$\Phi = \begin{pmatrix} \phi_1 \mathbf{1}_N & 0 \\ 0 & \phi_2 \mathbf{1}_N \end{pmatrix}. \quad (13)$$

With these basic elements the scattering matrix for multiple Andreev reflection at the interfaces, in combination with the intermediate propagation through the disordered region, takes the form<sup>11</sup>

$$\begin{aligned} \mathbf{S}_{\text{SNS}} &= \begin{pmatrix} e^{i(\varphi-\Phi)/2} & 0 \\ 0 & e^{i(\varphi+\Phi)/2} \end{pmatrix} \mathbf{S}_{\text{N}}(E) [\mathbf{1}_{4N} - \mathbf{S}_{\text{N}}^\dagger(E) \mathbf{S}_{\text{A}}(E)] \\ &\quad [\mathbf{1}_{4N} - \mathbf{S}_{\text{A}}(E) \mathbf{S}_{\text{N}}(E)]^{-1} \begin{pmatrix} e^{-i(\varphi-\Phi)/2} & 0 \\ 0 & e^{-i(\varphi+\Phi)/2} \end{pmatrix} \end{aligned} \quad (14)$$

where  $\mathbf{1}_{4N}$  is the  $4N \times 4N$  unit matrix. Obviously, the  $\varphi_j$  defined in (12) are real for  $E < \min\{\Delta_1, \Delta_2\} \equiv \Delta_{\min}$ . In this case, the matrix  $\mathbf{S}_{\text{A}}$  is unitary: Andreev reflection within the region between the two interfaces is current conserving. For  $|E| > \max\{\Delta_1, \Delta_2\} \equiv \Delta_{\max}$ , the matrix  $\mathbf{S}_{\text{A}}$  is hermitian, and only then is  $\mathbf{S}_{\text{SNS}}$  a unitary matrix.

### 2.3. Spectrum of States of a SNS-Junction

Corresponding to the range of energies at which we consider the electron propagation through the junction, we encounter three different regimes:

## M. Garst and T. Kopp

1.  $|E| > \Delta_{\max}$ , in which case we consider a continuum of particle and hole scattering states in each superconductor,
2.  $\Delta_{\max} > E > \Delta_{\min}$ , which is the intermediate regime with quasiparticle states extending over the superconductor with the lower energy gap but they decay exponentially in the superconductor with the larger gap,
3.  $|E| < \Delta_{\min}$ , in which case the BdG wave functions decay exponentially in both superconductors. Bound states, *Andreev states*, which are localized in the normal region, generate a discrete spectrum. For a finite phase difference,  $\phi = \phi_2 - \phi_1$ , Andreev states support an electrical current. Thereby, the coherent particle-hole excitations in the junction are converted into a supercurrent in the bulk superconductors.

### 2.3.1. Continuum states

In order to obtain the spectrum in this regime, one makes use of the “Wigner time-delay matrix”<sup>27,28</sup>  $\mathbf{S}^\dagger \frac{\partial}{\partial E} \mathbf{S}$ , the trace of which is the density of states,  $\rho(E)$ :

$$\rho(E) = \frac{1}{2\pi i} \text{tr} \left\{ \mathbf{S}^\dagger \frac{\partial}{\partial E} \mathbf{S} \right\} = \frac{1}{2\pi i} \frac{\partial}{\partial E} \ln \det \mathbf{S}. \quad (15)$$

As the scattering matrix of the junction  $\mathbf{S}_{\text{SNS}}$  is unitary, one may evaluate the relation (15) with  $\mathbf{S} = \mathbf{S}_{\text{SNS}}$  and find, respecting the hermiticity of  $\mathbf{S}_A(E)$ ,

$$\rho(E) = -\frac{1}{\pi} \frac{\partial}{\partial E} \Im \ln Z(E) + \rho_0(E) \quad (16)$$

with  $Z(E)$  a complex function defined through

$$Z(E) = \det(\mathbf{1}_{4N} - \mathbf{S}_A(E)\mathbf{S}_N(E)). \quad (17)$$

The additive term

$$\rho_0(E) = \frac{1}{2\pi i} \frac{\partial}{\partial E} \ln \det \mathbf{S}_N \quad (18)$$

in the density of states (16) is independent of the phase difference  $\phi$  of the two superconductors and will not contribute to the Josephson current.

### 2.3.2. Intermediate regime

The determination of the density of states in this energy regime does not proceed parallel to that of  $\rho(E)$  with extended quasiparticle states in



### RMT: Distribution of Mesoscopic Supercurrents ...

both superconductors. The scattering matrix of the junction is not unitary for  $\Delta_{\max} > E > \Delta_{\min}$  since the quasiparticle states decay exponentially in the superconductor with the larger energy gap — we assume this to be the left superconductor in Fig. 1. However, we can define a reduced scattering matrix  $\mathbf{S}_{\text{int}}$  which connects only the incoming amplitudes from the right superconductor to the outgoing amplitudes of the right superconductor

$$\begin{pmatrix} d_e^+ \\ d_h^- \end{pmatrix} = \mathbf{S}_{\text{int}} \begin{pmatrix} d_e^- \\ d_h^+ \end{pmatrix}, \quad (19)$$

and the dimension of this scattering matrix is half that of  $\mathbf{S}_{\text{SNS}}$ . Since  $\mathbf{S}_{\text{int}}$  is unitary, we may use relation (15) for  $\mathbf{S} = \mathbf{S}_{\text{int}}$ . After some tedious algebra we arrive again at

$$\rho(E) = -\frac{1}{\pi} \frac{\partial}{\partial E} \Im \ln Z(E) + \tilde{\rho}_0(E) \quad (20)$$

with a  $\phi$ -independent additive term  $\tilde{\rho}_0$

$$\tilde{\rho}_0(E) = \frac{1}{2\pi i} \frac{\partial}{\partial E} \ln \det \mathbf{S}_{\text{N}} - \frac{\varphi_1(E)}{\pi}. \quad (21)$$

As already indicated, the scattering matrix for Andreev scattering  $\mathbf{S}_{\text{A}}(E)$  in  $Z(E)$  is hermitian for the continuum states but not so for the intermediate states, and expressions (16) and (20) are indeed quite distinct.

#### 2.3.3. Bound states

Since the Andreev states are evanescent in the superconductors, the matrix  $\mathbf{S}_{\text{A}}(E)$  is now unitary. It obeys the simple relation for bound states

$$\begin{pmatrix} b_e^+ \\ c_e^- \\ b_h^- \\ c_h^+ \end{pmatrix} = \mathbf{S}_{\text{A}}(E) \mathbf{S}_{\text{N}}(E) \begin{pmatrix} b_e^+ \\ c_e^- \\ b_h^- \\ c_h^+ \end{pmatrix} \quad (22)$$

Solutions exist if  $Z(E) = 0$  is fulfilled. In this regime the density of states can therefore be written as

$$\begin{aligned} \rho(E) &= \left| \frac{\partial Z}{\partial E} \right| \delta(Z(E)) = -\frac{1}{\pi} \frac{\partial Z}{\partial E} \Im \frac{1}{Z(E + i0)} \\ &= -\frac{1}{\pi} \frac{\partial}{\partial E} \Im \ln Z(E + i0) \end{aligned} \quad (23)$$

**M. Garst and T. Kopp**

## **2.4. Josephson Current**

The stationary current  $I$  through a SNS-junction is driven by the phase difference of the superconductors. It can be obtained from a free energy  $F$  through the well-known thermodynamic relation

$$I = \frac{2e}{\hbar} \frac{dF}{d\phi}. \quad (24)$$

As elaborated in the literature (for example, see Ref. (11)) the current is given in terms of the density of quasiparticle states

$$I = -\frac{2e}{\hbar} 2k_B\tau \int_0^\infty dE \ln [2 \cosh (E/2k_B\tau)] \frac{d}{d\phi} \rho(E). \quad (25)$$

After an integration by parts the current can be expressed as

$$I = \frac{2e}{\pi\hbar} \int_0^\infty dE \tanh [E/2k_B\tau] j(E + i0, \phi), \quad (26)$$

where  $j$  is a kind of spectral current

$$\begin{aligned} j(E, \phi) &= -\frac{d}{d\phi} \Im \ln Z(E) \\ &= -\frac{d}{d\phi} \Im \ln \det(\mathbf{1}_{4N} - \mathbf{S}_A(E)\mathbf{S}_N(E)). \end{aligned} \quad (27)$$

This compact expression for the supercurrent is the basis for the calculation of the distribution of supercurrents through chaotic junctions in the following sections.

## **3. SINGLE CHANNEL CASE**

Quantum transport of coherent particle-hole excitations through a single channel is rather particular. Level repulsion is missing by construction. The transmission eigenvalues  $T$  are distributed according to a “single-particle” potential which is either logarithmically diverging for small  $T$  ( $\beta = 1$ ) or constant ( $\beta = 2$ ),  $P(T) = \frac{\beta}{2} T^{-1+\beta/2}$ . This potential will control the distribution of the critical currents. It should be realized that this scenario applies also for junction geometries where (many) different channels are uncoupled.

It is quite instructive to derive step by step the spectral current for this single channel case since the procedure conveys an understanding of the

### RMT: Distribution of Mesoscopic Supercurrents ...

validity and consequences of the approximations made. Here we present the result for the case of a scattering matrix which is energy independent, that is, the Thouless energy is much larger than  $\Delta_{\text{max}}$ , and there are no resonances at or in the gap. The following relation holds

$$j(E, \phi) = -\frac{d}{d\phi} \Im \ln [\cos(\varphi_1(E) + \varphi_2(E)) - R \cos(\varphi_1(E) - \varphi_2(E)) - T \cos \phi_{\text{eff}}], \quad (28)$$

which is derived in Appendix A where we also discuss an expansion in  $E/E_F$  of the phases of the scattering matrix. In the above expression, we introduced  $R = 1 - T$  and  $\phi_{\text{eff}} = \phi + \Delta\phi$ , where  $\Delta\phi$  is a phase which is generated from the phase factors  $U, U'$  and  $V, V'$  in the polar decomposition (3). Since  $\Delta\phi$  builds only on a difference of the respective phases, it is zero for the COE where  $U' = U^T$  and  $V' = V^T$  hold, whereas it runs from 0 to  $2\pi$  for the CUE.

We now restrict our discussion to symmetric contacts with  $\Delta_1 = \Delta_2 = \Delta$ . The energy eigenvalues for the Andreev states are straightforwardly found from the zeros of the logarithm in (28),  $E(\phi) = \pm \Delta \sqrt{1 - T \sin^2 \frac{\phi}{2}}$ . The supercurrent (26) is carried only by the Andreev states (the continuum contributions cancel):<sup>29</sup>

$$I(\phi, T) = \frac{e\Delta}{2\hbar} \frac{T \sin \phi}{\sqrt{1 - T \sin^2 \frac{\phi}{2}}} \tanh\left(\frac{\Delta}{2k_B T} \sqrt{1 - T \sin^2 \frac{\phi}{2}}\right). \quad (29)$$

Obviously, this expression recovers the well known sine-phi dependence for small transmission coefficients,  $I(\phi) = \frac{\pi\Delta}{2e} G \sin \phi$ , with the conductance  $G = 2e^2 T/h$ .

Finally, the current for a particular junction (29), characterized by a specific  $T$ , is averaged with the distribution function (5) for a single channel and we find for  $\tau = 0$  and  $\beta = 1$  (see Fig. 2, lowest curve)

$$\langle I(\phi) \rangle_{\text{COE}} = \frac{e\Delta}{\hbar} \sin \phi \frac{\phi - \sin \phi}{8 \sin^3 \frac{\phi}{2}} \quad \text{for } \phi \in [-\pi, \pi] \quad (30)$$

For  $\beta = 2$ , the phase difference  $\phi$  in (29) has to be replaced by  $\phi_{\text{eff}}$ . Integration over  $d\mu(U_\alpha)$  (see Eq. (4)) corresponds to averaging over  $\Delta\phi$  which results in a zero ensemble-averaged supercurrent for the CUE.

Moreover, the variance of the supercurrent can be calculated analytically. However we want to focus on a different issue: the critical current, that is, the maximum supercurrent is usually more accessible in experiments. In the single-channel case the structure of the supercurrent-phase relation (29) is actually so elementary for zero temperature that it is possible to determine

**M. Garst and T. Kopp**

	CUE	COE
$P(T)$	1	$\frac{1}{2\sqrt{T}}$
$\rho(i_c)$	$2(1 - i_c)$	$\frac{(1 - i_c)}{\sqrt{i_c(2 - i_c)}}$
$\langle i_c \rangle$	$\frac{1}{3}$	$1 - \frac{\pi}{4}$
$\text{var } i_c$	$\frac{1}{18}$	$\frac{2}{3} - \frac{\pi^2}{16}$

**Table 1.** *Distribution of the critical currents for the CUE and COE; the average critical current is  $\langle i_c \rangle = \int_0^1 i_c \rho(i_c)$ , and the variance is defined as  $\text{var } i_c = \langle i_c^2 \rangle - \langle i_c \rangle^2$ .*

directly the distribution function for the critical current. The distribution function  $\rho(i_c)$  for the dimensionless critical current,  $i_c = I_c / \frac{e\Delta}{\hbar}$ , characterizes the ensemble in a unique way, as we will present below. A suitable definition of the distribution function for the critical current is

$$\rho(i_c) = \int_0^1 dT P(T) \delta(i(T, \phi_c(T)) - i_c). \quad (31)$$

The critical current for a specific transmission coefficient,  $i(T, \phi_c)$ , is found from (29) (at  $\tau = 0$ ) together with the condition  $di(\phi_c, T)/d\phi_c = 0$ . It yields an implicit equation for  $\phi_c$  which reads  $T = T_c(\phi_c) = -\cos \phi_c / \sin^4 \frac{\phi_c}{2}$ . This latter relation allows to express the critical current in terms of  $\phi_c$ : it reads  $i(T_c(\phi_c), \phi_c) = 1 - (\tan \frac{\phi_c}{2})^{-2}$ . Since the function  $T_c(\phi_c)$  is monotonic and maps the interval  $[\pi/2, \pi]$  onto the interval  $[0, 1]$  we may rewrite the integral (31) in terms of an integration over  $\phi_c$ . Finally, making use of  $T_c(\phi_c) = i_c(2 - i_c)$ , we find the fundamental zero temperature relation for the distribution of the critical current:

$$\rho(i_c) = 2(1 - i_c) P(i_c(2 - i_c)). \quad (32)$$

Again,  $i_c$  is normalized to the maximum physical critical current  $e\Delta/\hbar$ , so it covers the interval  $[0, 1]$ . We would like to emphasize that this formula is valid in the presence as well as in the absence of time-reversal symmetry. For the single-channel case breaking of time-reversal symmetry results in a

## RMT: Distribution of Mesoscopic Supercurrents ...

shift of the  $I(\phi)$  curve by a constant phase  $\Delta\phi$  which does not affect the critical current.

The immediate consequences for the COE and CUE are summarized in Table 1. Relation (32) allows to determine the type of ensemble if the distribution of critical currents is measured. The distribution function for the COE diverges as  $1/\sqrt{i_c}$  for  $i_c \rightarrow 0$  (which is also displayed in Fig. 3,  $N = 1$ ), whose origin is the square root divergence of the distribution function  $P(T)$ .

## 4. MULTIPLE CHANNEL JUNCTIONS

Only in the presence of time-reversal symmetry,  $\beta = 1$ , the expression (28) for the spectral current can be generalized to multiple channels,

$$j(E, \phi) = - \sum_{n=1}^N \frac{d}{d\phi} \Im \ln [\cos(\varphi_1(E) + \varphi_2(E)) - R_n \cos(\varphi_1(E) - \varphi_2(E)) - T_n \cos \phi]. \quad (33)$$

In Appendix B the averaged critical supercurrent for the asymmetric Josephson junction is computed from this expression. For the symmetric junction,  $\Delta_1 = \Delta_2 = \Delta$ , again only the Andreev-states contribute and the current is given as a linear statistic as obtained by Beenakker,<sup>11</sup>

$$I(\phi, \{T_i\}) = \frac{e\Delta}{\hbar} \sum_{n=1}^N \frac{T_n \sin \phi}{2\sqrt{1 - T_n \sin^2 \frac{\phi}{2}}} \tanh\left(\frac{\Delta}{2k_B\tau} \sqrt{1 - T_n \sin^2 \frac{\phi}{2}}\right). \quad (34)$$

The average supercurrent can be determined analytically in the limit of large channel number  $N$  and zero temperature.<sup>23</sup> It is obtained with the density of transmission coefficients,  $\rho(T) = N/\pi [T(1 - T)]^{-1}$ , and is non-sinusoidal due to its dependence on the hypergeometric function  ${}_2F_1$ ,

$$\langle I(\phi) \rangle_{\text{COE}} = N \frac{e\Delta}{4\hbar} {}_2F_1\left(\frac{1}{2}, \frac{3}{2}, 2, \sin^2 \frac{\phi}{2}\right) \sin \phi \quad \text{for } N \rightarrow \infty. \quad (35)$$

This expression, valid for large  $N$ , is to be compared to results for finite  $N$ . For this purpose, the average supercurrent has been evaluated numerically for  $N = 1$  to  $N = 5$ . Although the curves do not scale with  $N$ —the maxima are slightly shifted with increasing  $N$  towards higher values of  $\phi$  (see Fig. 2a)—the overall shape of the supercurrent-phase relation is remarkably similar for  $N = 1$  to  $N = \infty$ . The same holds, to a lesser extent, for the root-mean-square (rms) fluctuations (Fig. 2b). For  $N = \infty$ , we included the result obtained by Beenakker,<sup>30</sup> which is slowly approached by the finite- $N$  results. He argued that corrections in  $1/N$  should move the finite value of rms  $I_{N=\infty}(\phi = \pi) = e\Delta/\pi\hbar$  to zero.

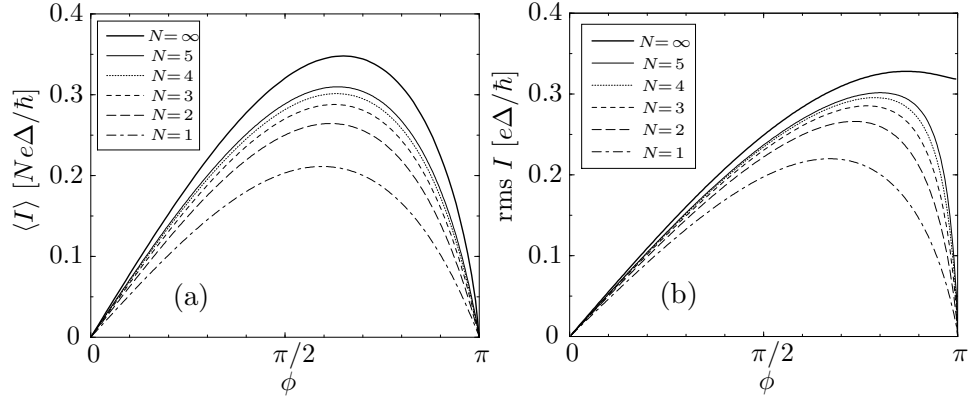


Fig. 2. Average supercurrent for the COE, scaled with  $Ne\Delta/\hbar$ , as a function of the phase difference  $\phi$  across the junction (a), and the rms fluctuations of the supercurrent, also for the COE (b).

Much more pronounced is the channel-number dependence of the distribution function for the critical current. The divergence of the distribution function in the COE is lifted in the multiple-channel situation due to the interaction between the transmission eigenvalues, that is, due to level repulsion. It is not possible to derive a closed expression for the distribution in the case of two or more channels. However, an analytical expression can be found which controls the limit  $i_c \rightarrow 0$ . The proof exploits again the simplicity of the current-phase relation (34) where we restrict the evaluation to zero temperature. The limit  $i_c \rightarrow 0$  is approached when all  $T_n \rightarrow 0$ . In this case, we neglect the square-root denominator, which results in  $\phi_c \rightarrow \pi/2$ . As expected, the critical current is in this limit proportional to the conductance  $g$ , i.e. the sum over all transmission eigenvalues,  $i(\phi_c, \{T_i\}) = \frac{1}{2} \sum_{n=1}^N T_n = \frac{1}{2}g$ . Therefore, for small  $i_c$ , the distribution of the critical current behaves in the same manner as the distribution of the conductance does.<sup>23</sup>

Similar to the single-channel situation, the distribution function for the critical current is defined as

$$\rho(i_c) = c_N^{-1} \prod_l \int_0^1 dT_l \prod_{n < m} |T_n - T_m| \prod_k T_k^{-1/2} \delta(i(\phi_c(\{T_i\}), \{T_i\}) - i_c) \quad (36)$$

After rescaling all transmission coefficients in (36) with  $i_c$  one obtains the

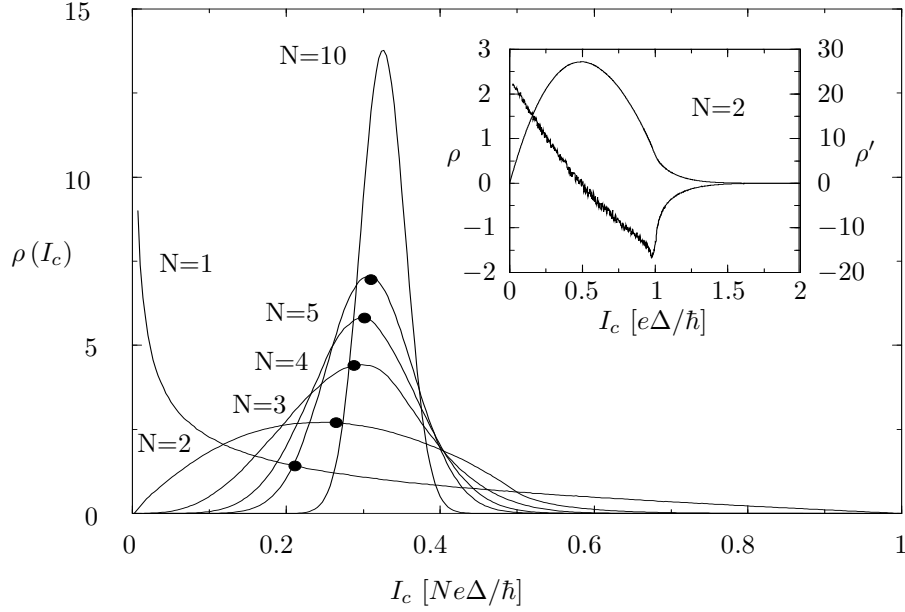


Fig. 3. Distribution function for the critical current in the COE for various channel numbers  $N$ . The maximum value reached by the averaged  $\langle I(\phi) \rangle$  (Fig. 2a) curve has been marked in the graph with the corresponding channel number by a black dot. The inset shows the distribution for  $N = 2$  and its derivative.

limiting small-current behavior

$$\rho(i_c \rightarrow 0) \sim i_c^\alpha \quad \text{with} \quad \alpha = \frac{N^2}{2} - 1 \quad (37)$$

For a single channel,  $N = 1$ , this agrees with the result of Table 1. In particular for two channels one obtains

$$\rho(i_c \rightarrow 0) \sim i_c \quad \text{for} \quad N = 2. \quad (38)$$

Level repulsion is responsible for the vanishing distribution function in the limit of zero critical current.

The distribution functions for the full range of  $i_c$  are generated numerically via a Monte Carlo integration. The results are displayed in Fig. 3. The numerical error is of the order of the line width. The distribution for  $N = 2$  again is shown in the inset together with its derivative. The derivative indicates clearly the feature at  $I_c = e\Delta/\hbar$ . For larger channel number  $N$ , the distribution functions approach a Gaussian distribution. In the limit  $N \rightarrow \infty$ , the Gaussian is characterized by  $\langle I_c \rangle = 0.35 Ne\Delta/\hbar$  and rms  $I_c = 0.30 e\Delta/\hbar$ ,

## M. Garst and T. Kopp

and the critical phase, at which the supercurrent attains its maximum value, is  $\phi_c = 2.04$ . For  $N = 10$  we are already close to this limit, with first moments  $\langle I_c \rangle = 0.33 \pm 0.01 N e \Delta / \hbar$  and rms  $I_c = 0.29 \pm 0.05 e \Delta / \hbar$ .

## 5. SUMMARY

The distribution function for the dimensionless critical current  $i_c = I_c / (e \Delta / \hbar)$  through a chaotic quantum dot is, for a large number of channels  $N$ , a Gaussian.<sup>11</sup> Its position is the average critical current of order  $N$  and its width are the root-mean-square fluctuations of  $i_c$  of order unity. With decreasing channel number these two first moments of the distribution function are still of order  $N$  and 1, respectively, however the prefactors change. Both, the average value of the critical current, normalized to  $N$ , and the rms fluctuations of the critical current decrease. This is not unexpected since the “level repulsion” between the transmission eigenvalues of different channels declines.

In the extreme case of a purely one-dimensional normal conducting contact, that is a single-channel contact, level repulsion is entirely absent and for the COE the distribution function displays a square-root divergence. This originates in the singular behavior of the distribution function for the transmission eigenvalues for the COE. Moreover, a general relation was established which connects the distribution of transmission eigenvalues to the distribution function for the critical supercurrent in the single channel situation. For multiple channels we provided a small current expansion of this distribution function which relates the number of channels to the exponent of the algebraic small-current behavior. With these relations it is in principle possible to identify the ensemble by a measurement of the distribution of critical currents.

## Acknowledgements

We acknowledge many helpful discussions with J.C. Cuevas, A. Mildenberger, A.D. Mirlin, A. Rosch and E. Scheer. Special thanks go to P. Wölfle who proposed the numerical determination of the distribution of the critical current. We dedicate this paper with great pleasure to Peter Wölfle on the occasion of his 60th birthday. This work was supported by the SFB 195 and by the BMBF 13N6918/1.



## APPENDIX A

Here, we elaborate on the determination of the spectral current  $j(E, \phi)$ , Eq. (27), for the single channel situation. An understanding of the energy dependence in this most simple case is useful for further discussions. The typical energy scale for variations of the scattering matrix elements is the Thouless energy.

The scattering matrix  $\mathcal{S}$  for the normal region of the contact is a  $2 \times 2$  matrix. In the polar decomposition (3) it is characterized by four phases  $\theta_L, \theta_R, \chi_L, \chi_R$  and the transmission coefficient  $T$  of this single channel:

$$\mathcal{S} = \begin{pmatrix} e^{i\theta_L} & 0 \\ 0 & e^{i\chi_L} \end{pmatrix} \begin{pmatrix} -\sqrt{1-T} & \sqrt{T} \\ \sqrt{T} & \sqrt{1-T} \end{pmatrix} \begin{pmatrix} e^{i\theta_R} & 0 \\ 0 & e^{i\chi_R} \end{pmatrix} \quad (39)$$

In general, these five parameters of the scattering matrix are energy dependent. We define the new phase parameters  $\theta = \theta_L + \theta_R$ ,  $\Delta\theta = \theta_L - \theta_R$ ,  $\chi = \chi_L + \chi_R$  and  $\Delta\chi = \chi_L - \chi_R$  and find for the spectral current

$$\begin{aligned} j(E, \phi) = & -\frac{d}{d\phi} \Im \ln [\cos(\varphi_1(E) + \varphi_2(E) - \frac{1}{2}(\theta(E) - \theta(-E) + \chi(E) - \chi(-E))) \\ & - \bar{R}(E) \cos(\varphi_1(E) - \varphi_2(E) - \frac{1}{2}(\theta(E) - \theta(-E) - \chi(E) + \chi(-E))) \\ & - \bar{T}(E) \cos(\phi + \frac{1}{2}(\Delta\theta(E) + \Delta\theta(-E) - \Delta\chi(E) - \Delta\chi(-E)))] \end{aligned} \quad (40)$$

with the particle-hole symmetric values for transmission and reflection coefficients

$$\begin{aligned} \bar{T}(E) &= \sqrt{T(E)T(-E)} \\ \bar{R}(E) &= \sqrt{(1-T(E))(1-T(-E))}. \end{aligned} \quad (41)$$

If the matrix  $\mathcal{S}$  is only weakly energy dependent (in particular no resonances should exist in an energy range of  $2\Delta$  around the Fermi energy  $E_F$ ) the above expression can be expanded: according to the Andreev approximation the phases are taken to first order in  $E/E_F$  and the transmission coefficient in zeroth order. This results in the low-energy expression for the spectral current

$$\begin{aligned} j(E, \phi) = & -\frac{d}{d\phi} \Im \ln [\cos(\varphi_1(E) + \varphi_2(E) - (\theta'(0) + \chi'(0))E) \\ & - R \cos(\varphi_1(E) - \varphi_2(E) - (\theta'(0) - \chi'(0))E) \\ & - T \cos(\phi + \Delta\theta(0) - \Delta\chi(0))] \end{aligned} \quad (42)$$

where the prime on the phases denotes a derivative with respect to energy, and  $R = 1 - T$ .

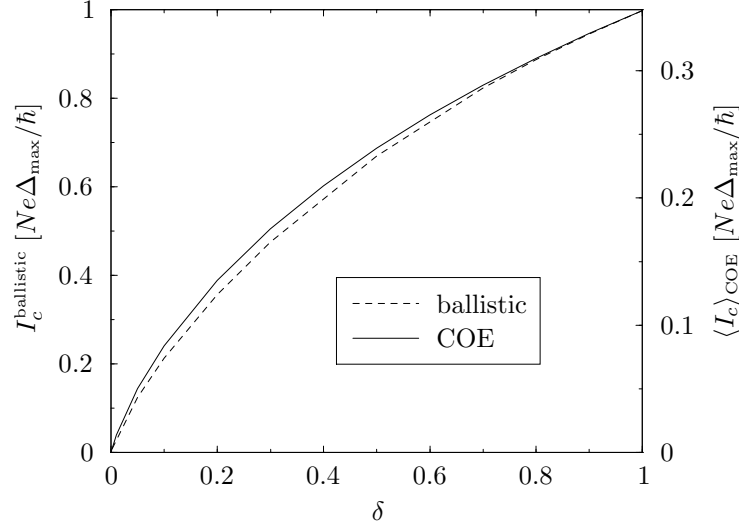


Fig. 4. Critical current for large  $N$  of an asymmetric Josephson contact averaged over the COE and of a ballistic contact for different ratios  $\delta = \Delta_{\min}/\Delta_{\max}$ .

Only in the presence of time-reversal symmetry the phases  $\Delta\theta(0)$  and  $\Delta\chi(0)$  vanish. However, in the absence of time-reversal symmetry the whole  $I(\phi)$  curve is shifted by  $\Delta\theta(0) - \Delta\chi(0)$ . The mean supercurrent at a fixed phase  $\phi$  then requires averaging over the constant phase shift which results in a vanishing supercurrent. On the other hand, a measurement of only the critical current is not affected by this phase shift and therefore expression (32) is valid irrespective of the presence or absence of time-reversal symmetry.

Assuming the transmission coefficients to be distributed according to the COE, the averaged spectral current (42) reads in the presence of time-reversal symmetry

$$\langle j(E, \phi) \rangle_{\text{COE}} = \Im \left\{ \frac{\sin \phi}{\cos \phi - \cos(\varphi_1 - \varphi_2 - (\theta' - \chi')E)} \left( 1 - \frac{\arctan \sqrt{a}}{\sqrt{a}} \right) \right\} \quad (43)$$

where

$$a = \frac{\cos(\varphi_1 - \varphi_2 - (\theta' - \chi')E) - \cos \phi}{\cos(\varphi_1 + \varphi_2 - (\theta' + \chi')E) - \cos(\varphi_1 - \varphi_2 - (\theta' - \chi')E)}. \quad (44)$$

The derivatives of the phases are taken at  $E = 0$ . The averaged spectral current (43) can be considered as a basis for a more detailed evaluation

## RMT: Distribution of Mesoscopic Supercurrents ...

respecting a weak energy dependence of the scattering matrix.

If we neglect the energy dependence of the scattering matrix altogether, we arrive at Eq. (28), which was the basic equation for the evaluation in the section on single channel junctions.

## APPENDIX B

In the limit of a large number of channels  $N$  the expression (33) for the spectral current of an asymmetric Josephson junction can be averaged over the COE with the distribution  $\rho(T) = N/\pi [T(1-T)]^{-1}$ . We get

$$\langle j(E, \phi) \rangle = \Im \left\{ \frac{N \sin \phi}{\cos \phi - \cos(\varphi_1 - \varphi_2)} \left( 1 - \left[ 1 + \frac{\cos(\varphi_1 - \varphi_2) - \cos \phi}{\cos(\varphi_1 + \varphi_2) - \cos(\varphi_1 - \varphi_2)} \right]^{-1/2} \right) \right\}. \quad (45)$$

The averaged critical current  $\langle I_c \rangle$  for large  $N$  can now be evaluated numerically and is shown in Fig. 4 versus the asymmetry parameter  $\delta = \Delta_{\min}/\Delta_{\max}$ . For  $\delta = 1$  it starts at the value  $\langle I_c \rangle = 0.35 Ne\Delta/\hbar$  for the symmetric junction and decreases with decreasing  $\delta$ . For comparison the values of  $I_c$  for the ballistic junction with  $N$  open channels are also shown.

## REFERENCES

1. B.L. Al'tshuler, P.A. Lee, and R.A. Webb, eds., *Mesoscopic Phenomena in Solids* (North-Holland, Amsterdam, 1991), and references therein.
2. Y. Imry, *Introduction to Mesoscopic Physics*, (Oxford University Press, 1997).
3. For an extended discussion of mesoscopic Josephson effects see: *Proceedings of the NATO Advanced Research Workshop on Mesoscopic Superconductivity*, eds. F.W.J. Hekking, G. Schön and D.V. Averin (1994, North-Holland, Amsterdam, or *Physica* **203B**, Nos. 3 & 4).
4. B.L. Al'tshuler, *Pis'ma Zh. Eksp. Teor. Fiz.* **41**, 530 (1985) [*JETP Lett.* **41**, 648 (1985)].
5. P.A. Lee and A.D. Stone, *Phys. Rev. Lett.* **55**, 1622 (1985).
6. Muttalib, Pichard, and Stone, *Phys. Rev. Lett.* **59**, 2475 (1987).
7. P.A. Mello, P. Pereyra, and N. Kumar, *Ann. Phys. (N.Y.)* **181**, 290 (1988).
8. Y. Imry, *Europhys. Lett.* **1**, 249 (1986).
9. S. Washburn and R.A. Webb, *Adv. Phys.* **35**, 375 (1986).
10. C.W.J. Beenakker, *Phys. Rev. Lett.* **67**, 3836 (1991) and *Phys. Rev. Lett.* **68**, 1442 (E) (1992).
11. C.W.J. Beenakker, *Three "universal" mesoscopic Josephson effects in: Proc. 14th Taniguchi Int. Symp. on 'Physics of Mesoscopic Systems'*, eds. H. Fukuyama and T. Ando (Springer, Berlin, 1992).

**M. Garst and T. Kopp**

12. A heterogeneous SNS-junction consists of two superconductors with different values of the superconducting gap,  $\Delta_1 \neq \Delta_2$ , whereas for a homogeneous junction  $\Delta_1 = \Delta_2$ .
13. A. F. Andreev, *Zh. Eksp. Teor. Fiz.* **46**, 1823 (1964); **49**, 655 (1965) [*Sov. Phys. JETP* **19**, 1228 (1964); **22**, 455 (1966)].
14. A quantity  $A = \sum_n a(T_n)$  is denoted a linear statistic on the transmission coefficients because products of  $T_n$  are absent.
15. C.W.J. Beenakker, *Rev. Mod. Phys.* **69**, 3 (1997).
16. P.W. Brouwer and C.W.J. Beenakker, *Chaos, Solitons & Fractals* **8**, 1249 (1997).
17. H.D. Politzer, *Phys. Rev. B* **40**, 11917 (1989).
18. E. Scheer, W. Belzig, Y. Naveh, M.H. Devoret, D. Esteve, and C. Urbina, *Phys. Rev. Lett.* **86**, 284 (2001).
19. M.F. Goffman, R. Cron, A. Levy Yeyati, M.H. Devoret, D. Esteve, and C. Urbina, *Phys. Rev. Lett.* **85**, 170 (2000).
20. M.C. Koops, G.V. van Duynveldt and R. de Bruyn Ouboter, *Phys. Rev. Lett.* **77**, 2542 (1996); mechanically controllable break junctions, which are indeed atomic-size quantum point contacts, were developed first by C.J. Muller, J.M. van Ruitenbeek and L.J. de Jongh, *Physica* **191C**, 485 (1992).
21. S. Kirchner, J. Kroha, and E. Scheer, *Generalized conductance sum rule in atomic break junctions* in: *Proc. of the NATO Advanced Research Workshop 'Size dependent magnetic scattering'*, Pecs, Hungary, May 28 - June 1, 2000, in press (Kluwer Academic Publishers, 2001); cond-mat/0010103.
22. Th. Martin and R. Landauer, *Phys. Rev. B* **45**, 1742 (1992).
23. H.U. Baranger and P.A. Mello, *Phys. Rev. Lett.* **73**, 142 (1994).
24. R.A. Jalabert, J.-L. Pichard, and C.W.J. Beenakker, *Europhys. Lett.* **27**, 255 (1994).
25. K. Böttcher and T. Kopp, *Phys. Rev. B* **55**, 11670 (1997).
26. K.K. Likharev, *Rev. Mod. Phys.* **51**, 101 (1979).
27. M.L. Goldberger and K.M. Watson, *Collision Theory* (John Wiley & Sons, 1964).
28. E. Doron and U. Smilansky, *Phys. Rev. Lett.* **68**, 1255 (1992).
29. W. Haberkorn, H. Knauer, and J. Richter, *Phys. Status Solidi A* **47**, K161 (1978).
30. C.W.J. Beenakker, *Phys. Rev. B* **47**, 15763 (1993).